Link Between GIP and Osteopontin in Adipose Tissue and Insulin Resistance

Emma Ahlqvist,[1] Peter Osmark,[1] Tiina Kuulasmaa,[2] Kasper Pilgaard,[3] Bilal Omar,[4] Charlotte Brøns,[3] Olga Kotova,[5] Anna V. Zetterqvist,[5] Alena Stančáková,[6] Anna Jonsson,[1] Ola Hansson,[1] Johanna Kuusisto,[6] Timothy J. Kieffer,[7,8] Tiinamaija Tuomi,[9,10] Bo Isomaa,[9,11] Sten Madsbad,[12] Maria F. Gomez,[5] Pernille Poulsen,[3] Markku Laakso,[6] Eva Degerman,[4] Jussi Pihlajamäki,[2,6] Nils Wierup,[13] Allan Vaag,[3,14] Leif Groop,[1,15] and Valeriya Lyssenko[1]

Low-grade inflammation in obesity is associated with accumulation of the macrophage-derived cytokine osteopontin (OPN) in adipose tissue and induction of local as well as systemic insulin resistance. Since glucose-dependent insulinotropic polypeptide (GIP) is a strong stimulator of adipogenesis and may play a role in the development of obesity, we explored whether GIP directly would stimulate OPN expression in adipose tissue and thereby induce insulin resistance. GIP stimulated OPN protein expression in a dose-dependent fashion in rat primary adipocytes. The level of *OPN* mRNA was higher in adipose tissue of obese individuals (0.13 ± 0.04 vs. 0.04 ± 0.01, $P < 0.05$) and correlated inversely with measures of insulin sensitivity ($r = -0.24$, $P = 0.001$). A common variant of the GIP receptor (*GIPR)* (rs10423928) gene was associated with a lower amount of the exon 9–containing isoform required for transmembrane activity. Carriers of the A allele with a reduced receptor function showed lower adipose tissue *OPN* mRNA levels and better insulin sensitivity. Together, these data suggest a role for GIP not only as an incretin hormone but also as a trigger of inflammation and insulin resistance in adipose tissue. Carriers of the *GIPR* rs10423928 A allele showed protective properties via reduced GIP effects. Identification of this unprecedented link between GIP and OPN in adipose tissue might open new avenues for therapeutic interventions. ***Diabetes*** **62:2088–2094, 2013**

From the [1]Department of Clinical Sciences, Diabetes, and Endocrinology, University Hospital Malmö, Lund University, Malmö, Sweden; the [2]Department of Clinical Nutrition, University of Eastern Finland, Kuopio, Finland; the [3]Steno Diabetes Center, Gentofte, Denmark; the [4]Department of Experimental Medical Sciences, Lund University, Lund, Sweden; [5]Vascular ET-Coupling, Department of Clinical Sciences, University Hospital Malmö, Lund University, Malmö, Sweden; the [6]Department of Medicine, University of Eastern Finland and Kuopio University Hospital, Kuopio, Finland; the [7]Laboratory of Molecular and Cellular Medicine, Department of Cellular and Physiological Sciences, Life Sciences Institute, University of British Columbia, Vancouver, British Columbia, Canada; the [8]Department of Surgery, University of British Columbia, Vancouver, British Columbia, Canada; the [9]Folkhalsan Research Centre, Helsinki, Finland; the [10]Department of Medicine, Helsinki University Central Hospital, and Research Program of Molecular Medicine, University of Helsinki, Helsinki, Finland; the [11]Department of Social Services and Health Care, Jakobstad, Finland; the [12]Department of Endocrinology, Hvidovre Hospital, University of Copenhagen, Copenhagen, Denmark; the [13]Unit of Neuroendocrine Cell Biology, Department of Clinical Sciences, Lund University, Malmö, Sweden; the [14]Department of Endocrinology, Rigshospitalet and Copenhagen University, Copenhagen, Denmark; and the [15]Finnish Institute of Molecular Medicine, Helsinki University, Helsinki, Finland.

Corresponding author: Valeriya Lyssenko, valeriya.lyssenko@med.lu.se.

Received 20 July 2012 and accepted 7 January 2013.

DOI: 10.2337/db12-0976

This article contains Supplementary Data online at http://diabetes.diabetesjournals.org/lookup/suppl/doi:10.2337/db12-0976/-/DC1.

Low-grade inflammation is a hallmark of adipose tissue expansion in obesity, which is associated with an accumulation of macrophages and cytokines in the tissue (1). Furthermore, low-grade inflammation may play a causal role in the link between obesity and systemic insulin resistance. Cytokines produced and present in adipose tissue are often referred to as adipokines and include leptin, resistin, IL6, osteopontin (OPN), etc. OPN is one of the most abundant cytokines in adipose tissue of obese individuals (2,3), and expression of *OPN* showed large differences in adipose tissue between monozygotic twins discordant for obesity (3). OPN is a secreted glycoprotein containing an Arg-Gly-Asp-Ser sequence that can interact with integrins and CD44 receptors and recruit macrophages and T cells to inflammatory sites (4). Whereas mice fed a high-fat diet became obese and displayed increased circulating OPN concentrations, obese mice lacking OPN showed increased insulin sensitivity (2), thereby proposing OPN as a key player in high-fat diet–induced insulin resistance. Besides an effect on insulin, the incretin hormone glucose-dependent insulinotropic polypeptide (GIP) exerts strong effects on adipose tissue formation. GIP stimulates adipose tissue formation independently of its effect on insulin secretion (5), and inactivation of the GIP receptor (GIPR) in adipose tissue has been suggested as a strategy to treat obesity (6).

We have previously demonstrated that GIP stimulates expression of OPN in human islets where OPN exerts protection against cytokine-induced apoptosis (7). Also, a variant in the *GIPR* locus (single nucleotide polymorphism [SNP] rs10423928) was associated with impaired insulin secretion and decreased BMI, which was sufficient to ameliorate the risk of type 2 diabetes associated with impaired insulin secretion. Given the putative important role of GIP in adipose tissue biology as well as a suspected role of OPN in adipose tissue subclinical inflammation, we hypothesized that GIP may also stimulate the expression of OPN in adipose tissue and thereby induce insulin resistance. The aim of this study was thus to explore whether GIP effects on adipose tissue may also include stimulation of OPN and induction of insulin resistance, and whether this was influenced by a variant in the *GIPR* gene.

RESEARCH DESIGN AND METHODS

All human and animal protocols were approved by the local ethics committees and performed in accordance with local institutional and national regulations.

Study participants

Prevalence, Prediction, and Prevention of Diabetes. The PPP-Botnia Study (Prevalence, Prediction, and Prevention of Diabetes) is a population-based study from the Botnia region, which included ~7% of the population 18–75 years of age (mean age 51 ± 17 years) (8). The aim was to study the prevalence and presence of risk factors for diabetes, impaired glucose tolerance, and metabolic syndrome in the general population. Diagnosis of diabetes was confirmed from subject records or on the basis of a fasting plasma glucose concentration ≥7.0 mmol/L and/or 2-h glucose ≥11.1 mmol/L. Nondiabetic subjects (n = 4,532) were included in the current study.

Measurements. In the PPP-Botnia Study, blood samples were drawn at 0, 30, and 120 min of the oral glucose tolerance test (OGTT). Levels of human GIP (total) and OPN in plasma were assayed using the Quantikine GIP and OPN ELISA kit (Millipore; R&D Systems, Abingdon, U.K.) according to the manufacturer's instructions. Absorbance was measured at 450 nm and the lower limit of detection was 5.7 pg/mL.

Calculations. Insulin sensitivity index (ISI) from the OGTT was calculated as 10,000/$\sqrt{}$(fasting plasma glucose [mg/dL] × fasting insulin [μU/L] × mean $OGTT_{glucose}$ × mean $OGTT_{insulin}$) (9).

Subcutaneous and visceral fat from individuals undergoing bariatric surgery. Abdominal visceral adipose tissue (VAT) and subcutaneous adipose tissue (SAT) biopsies were available from 38 obese nondiabetic subjects undergoing bariatric surgery at Landskrona Hospital (Landskrona, Sweden) (5 men and 33 women; 36 (30–47) years of age; weight = 112 (102–124) kg; BMI = 41 ± 5 kg/m^2; total body fat mass = 68 ± 14 kg). Biopsies were immediately frozen in liquid nitrogen and stored at −80°C.

Danish Twins Study. Of 606 mono- and dizygotic same-sex twins previously participating in a population-based study (10,11), 298 elderly twins (mean age 74 ± 5 years) were examined with a standardized OGTT and anthropometric measurements. In this cohort, 57% were normal glucose tolerant, 27% had impaired glucose tolerance, and 16% had type 2 diabetes.

Measurements. In addition to an OGTT, a SAT biopsy was taken from the abdomen under local anesthesia using a Bergstrom needle, and the tissue was immediately frozen in liquid nitrogen and stored at −80°C.

Danish overfeeding study. Forty-eight young male volunteers born in 1979–1980 in Copenhagen were recruited from the Danish National Birth Registry (12). None of the participants had known illness or took medications known to affect the study outcome.

Indirect calorimetry. Basal and insulin-stimulated glucose and fat oxidation rates were calculated as GOX (g/min) = 4.55 × VCO_2 (L/min) − 3.21 × VO_2 (L/min) − 2.87 × n (g/min) and FOX = 1.67 × VO_2 (L/min) − 1.67 × VCO_2 (L/min) − 1.92 × n (g/min), where n is nitrogen secreted in the urine (13). Glucose and lipid oxidation are expressed as mg · kg FFM^{-1} · min^{-1}.

EUGENE2 Study. The participants included in this study were 110 healthy, nondiabetic offspring of patients with type 2 diabetes from the Kuopio center of the EUGENE2 Study (14). One of the parents had to have type 2 diabetes and the other parent normal glucose tolerance in an OGTT and/or no history of type 2 diabetes in the family. All these subjects (36.6 ± 6.0 years of age; BMI 25.9 ± 4.7 kg/m^2) underwent an adipose tissue needle biopsy from abdominal subcutaneous tissue as previously reported (15). All protocols were approved by the regional ethics committee, and procedures were performed according to the principles of the Helsinki Declaration. After thorough written and oral explanation of the study, all subjects gave their written consent.

Measurements of *GIPR* and *OPN* mRNA expression. mRNA levels were measured in adipose tissue (subcutaneous and visceral fat from Landskrona obese) by real-time quantitative RT-PCR (TaqMan Gene Expression Assays; Applied Biosystems) according to the manufacturer's protocols. RNA was isolated using the RNeasy Plus Minikit (Qiagen, Valencia, CA). Concentration and purity were measured using NanoDrop ND-1000 spectrophotometer (NanoDrop Technologies, Wilmington, DE). No sign of degradation was observed using agarose gel electrophoresis and Experion DNA 1-K gel chips (Bio-Rad, Hercules, CA). RNA (0.2–0.5 μg) was used for cDNA synthesis with RevertAid First Strand cDNA Synthesis Kit (Fermentas Life Sciences). TaqMan gene expression assays were purchased from Applied Biosystems. For human tissue, assay IDs were Hs00164732_m1 for GIPR and Hs00959010_m1 for OPN (SPP1). Target gene expression was normalized to the expression of the following housekeeping genes: human *HPRT1* (HGPRT, article no. 4326321E), human *PPIA* (cyclophilin A, article no. 4326316E), human *POLR2A* (POLR2A, article Hs00172187_m1). Q-PCR reactions were run on ABI 7900 HT (Applied Biosystems) using 5–10 ng cDNA, and all assays were run in triplicate (total volume of PCR reactions = 10 μL). Relative quantity of *GIPR* and *OPN* mRNA was calculated using the comparative threshold method, and normalization was performed using Genorm version 3.5 software.

Western blotting. Primary adipocytes were isolated from the epididymal fat pads of 36–42-day-old male Sprague-Dawley rats by collagenase digestion as previously described (16). Primary rat adipocytes (10% cell suspension) were suspended in serum-free Dulbecco's modified Eagle's medium supplemented with 0.5% BSA, 100 units/mL penicillin, and 100 μg/mL streptomycin. Adipocytes were transferred to six-well plates (1-mL cell suspension per well) and incubated at 37°C with 95% O_2/5% CO_2 for 2 h prior to addition of 100 nmol/L GIP or 1 nmol/L insulin alone or in combination. After an overnight (~18 h) incubation with the hormones, cells were washed with Krebs-Ringer-HEPES buffer containing 25 mmol/L HEPES, 200 nmol/L adenosine, and 2 mmol/L glucose prior to lysis in a buffer containing 50 mmol/L N-[tris(hydroxymethyl) methyl]-2-aminoethanesulfonic acid (TES), 2 mmol/L EGTA, 1 mmol/L EDTA, 250 mmol/L sucrose, 40 mmol/L phenylphosphate, 5 mmol/L NaF, 1 mmol/L dithioerythriol, 0.5 mmol/L sodium orthovanadate, 10 μg/mL antipain, 10 μg/mL leupeptin, 1 μg/mL pepstatin A, and 1% Nonidet P40. Protein was determined by Bradford assay. Aliquots of the cell lysates (20 μg) were mixed with Laemmli sample buffer, separated on 12% polyacrylamide gels, and subsequently transferred to nitrocellulose membranes (Amersham Biosciences, Buckinghamshire, U.K.). After blocking in 3% BSA/5% nonfat dry milk, membranes were incubated with primary antibody against OPN (1 μg/mL; Developmental Studies Hybridoma Bank, Iowa City, IA) and horseradish peroxidase (HRP)-conjugated secondary antibody (Amersham Biosciences), and bands were detected with Supersignal West Pico ECL reagents (Pierce Biotechnology, Rockford, IL). Western blots were quantified using Image Gauge software (Fujifilm).

Splicing analysis

Subjects and RNA extraction. A total of 110 nondiabetic offspring of type 2 diabetic patients (36.6 ± 6.0 years of age, BMI = 25.9 ± 4.7 kg/m^2) from the Kuopio center of the EUGENE2 Study (14) underwent an adipose needle biopsy from abdominal subcutaneous tissue. Total RNA from biopsies was isolated using Trizol reagent (Invitrogen, Carlsbad, CA) and Qiagen RNeasy Minikit (Ambion, Austin, TX) and transcribed to cDNA using random primers and a high-capacity cDNA archive kit (Applied Biosystems). Quantitative RT-PCRs were performed in a 7,500 Real-Time PCR System (Applied Biosystems) using 6 ng (RNA equivalents) cDNA as template, gene-specific primers, and probes (information on primers and probes available upon request from Applied Biosystems). Target gene expression was normalized to large ribosomal protein P0 (Hs99999902_ml; Applied Biosystems) using the standard curve method.

Identification of GIPR splice variants. Analytical RT-PCRs were performed on cDNA from visceral fat and subcutaneous fat in 15-μL reactions using 7.5 μL AmpliTaq Gold PCR Master Mix (Applied Biosystems, Foster City, CA) supplemented with 0.75 μL DMSO and 1.5 μmol/L forward and reverse primer. The following primers were used in various combinations: exon1fw, GGCTGCAGGAGCAAGTGA; exon2fw, GATCGCCCCTGCACGAAC; exon5fw, TTGGAGAGACCATACACAATGTG; exon8fw, CTGCCTGCCGCACGGCCCAGAT; exon10fw, GGATTATACGGACCCCCATC; exon5rv, CACATTGTGTATGGTCTCTCCAA; exon8rv, GTTGGCACCCACGCAGTA; exon10rv, CAAATGGCCTTGACTTCGTTG; exon11rv, CGTGTCCTCAGCTTGGACA; and exon14rv, CGCCCCTAGCAGTAACTTTCC. The reactions were carried out with 60°C annealing temperature and >50 cycles. Products were analyzed on 2% agarose. Prior to sequencing, 2.5 μL PCR product was treated with 0.5 μL ExoSAP-IT (USB, Cleveland, OH) at 37°C for 30 min and deactivated at 80°C for 15 min. Subsequently, 1 μL was sequenced in both directions using BigDye 3.1 according to the manufacturer's protocol (Applied Biosystems, Foster City, CA). The sequence reactions were purified and analyzed by RSKC (Malmö, Sweden).

Quantitative analysis of alternative splicing between exons 8 and 10. For PCR reactions, 5 ng cDNA was added to PCR reaction mixture consisting of onefold PCR buffer, 200 μmol/L dNTPs, 150 μmol/L forward and reverse primers, and 0.4 units DyNAzyme II Hot Start DNA Polymerase (Finnzymes, Espoo, Finland). Primers were planned to span an alternatively spliced region resulting in PCR products that vary in size depending on splicing. For DNA fragment analysis, PCR products were diluted to avoid saturation of capillary electrophoresis (1:4 in water). One microliter of PCR product dilution was mixed with 10 μL HiDi formamide (ABI) and 0.4 μL of internal size standard GeneScan 600 LIZ (ABI; Applied Biosystems). Samples were denatured for 5 min at 95°C and then immediately placed on ice for at least 15 min. Samples were run on the ABI3100 DNA Genetic Analyzer (ABI), and the results were analyzed using Peak Scanner Software version 1.0 (ABI). Peak areas were used to calculate the relative quantities of the PCR products.

Detection of GIPR protein by immunohistochemistry

Human tissue. White adipose tissue (n = 20) was taken during obesity surgery from healthy volunteers. Adipose and skeletal muscle specimens were immediately fixed in 4% paraformaldehyde in 0.1 mol/L phosphate buffer (pH 7.2) at 4°C, rinsed in graded ethanols, embedded in paraffin, and sectioned (6 μm).

Animal tissue. For adipose and skeletal tissue, Sprague Dawley rats (n = 10) and C57Bl/6J mice (n = 10; Taconic Europe, Ry, Denmark) were used. Specimens were dissected out, fixed overnight in Stefanini's solution (2% paraformaldehyde and 0.2% picric acid in 0.1 mol/L PBS, pH 7.2), rinsed thoroughly in Tyrode's solution containing 10% sucrose, embedded, and cryosectioned (10 μm). Cell membranes were stained with CellMask (Invitrogen).

Immunofluorescence. Adipose and muscle tissue were stained as previously described (15). In brief, sections were boiled in 0.01 mol/L citrate buffer (pH 6.0) for 2 × 7 min at 650 W. Primary antibodies were diluted in PBS containing 0.25% BSA and 0.25% Triton X-100 and applied overnight at 4°C. Rabbit polyclonal anti-GIPr (1:1,600) (7,17) was used. Secondary antibodies specific for rabbit IgG and coupled to Cy2 (Jackson, West Grove, PA) were applied for 1 h at room temperature. Immunofluorescence was examined in an epifluorescence microscope (Olympus BX60). Images were taken with a digital camera (Nikon DS-2Mv).

Genotyping. Genotyping of rs10423928 was performed using matrix-assisted laser desorption ionization time of flight mass spectrometry on the Sequenom MassARRAY platform (San Diego, CA) for PPP-Botnia and using an allelic discrimination method with a TaqMan assay on the ABI 7900 platform (Applied Biosystems, Foster City, CA) for the Danish Twins Study and EUGENE2. We obtained an average genotyping success rate of >95.5% and an average concordance rate in all studies of >99.9%. Hardy-Weinberg equilibrium was fulfilled in all studied populations ($P > 0.50$).

Statistical analyses. Linear regression analyses were used to test genotype-phenotype correlations adjusted for age, sex, and BMI (apart from BMI). Nonnormally distributed variables were logarithmically (natural) transformed before analysis. Analyses were performed using SPSS version 17.0, PLINK, or STATA version 10. For in vitro studies, results were expressed as mean ± SEM, where applicable. Statistical analyses were performed using GraphPad (Prism 4.0) or Origin (Originlab), and significance was determined using unpaired two-tailed Student *t* test. *P* value <0.01 was considered statistically significant unless replicating previous findings, when the threshold was set at $P < 0.05$.

RESULTS

GIPR expression in adipose tissue. Expression of GIPR determined both by real-time PCR and immunostaining demonstrated that the GIPR protein was abundant in adipose tissue and skeletal muscle (Fig. 1*A* and Supplementary Fig. 1). Expression of *GIPR* mRNA was higher in visceral than in subcutaneous fat (mean ± SEM, 0.45 ± 0.04 vs. 0.28 ± 0.03, $P = 2.0 \times 10^{-6}$) in 30 obese nondiabetic subjects undergoing bariatric surgery. Circulating fasting plasma GIP concentrations were positively associated with BMI, and to a lesser extent with lean body mass (LBM) and fat (%) (BMI, $r = 0.054$, $P = 0.0003$; fat %, $r = 0.038$, $P = 0.045$; LBM, $r = 0.043$, $P = 0.023$), but negatively associated with insulin sensitivity (ISI) ($r = -0.096$,

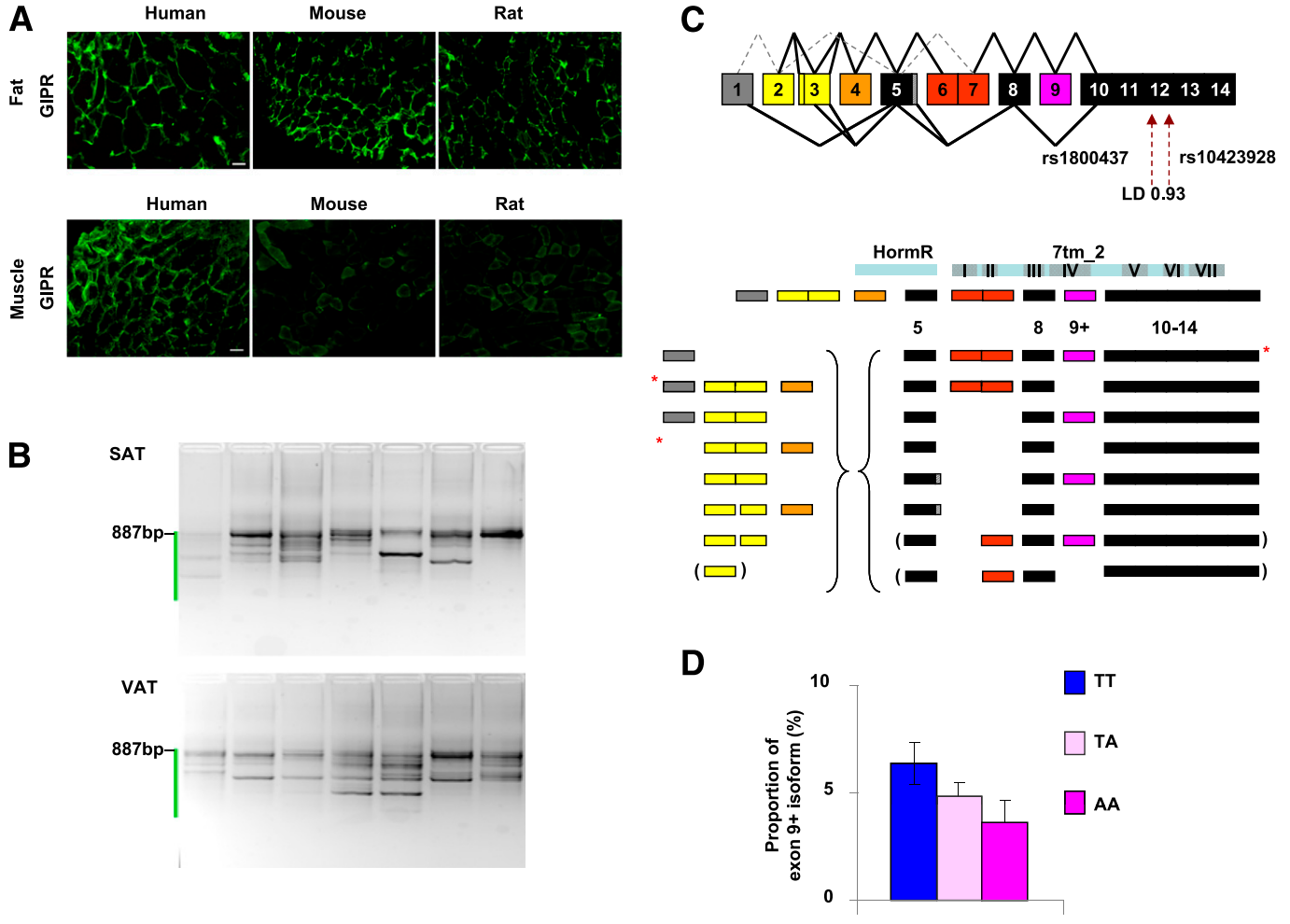

FIG. 1. Expression of the GIPR in adipose tissue. ***A*****: Immunostainings demonstrating that GIPR (green) is abundantly expressed in human, mouse, and rat white adipose tissue (*top*) and skeletal muscle (*bottom*). Scale bar, 50 μm.** ***B*****: Agarose gel electrophoresis of RT-PCR across the variable part of GIPR cDNA (from exon 2 to 10) from SAT and VAT samples from seven individuals. The size of the predicted functional GIPR amplicon of 887 bp is indicated, as well as the size range of identified splice variants (green bars).** ***C*****: Schematic representation of alternative splicing of the full-length GIPR. Black exons are obligatory and colored are variable. Dashed lines indicate rare events. Exon 1, which is noncoding, is presumably variable. Exons 3 and 5 possess alternative splice sites. The GIP binding site (HormR) and the transmembrane domain (7tm_2) are indicated. Transmembrane helices (gray) I, II, III, and VI are encoded by single exons. Splice variants were detected by RT-PCR and sequencing. Variants predicted to yield a fully functional membrane-bound GIPR are indicated by asterisks.** ***D*****: Proportion of full mRNA splice variants including exon 9 is decreased in the adipose tissue of subjects with the A allele of rs10423928 (ANOVA, $P < 0.05$). PCR primers are shown in exons 8 and 11. Variant ratios were detected using PCR and capillary electrophoresis. Peak areas were used to calculate the relative quantities of the PCR products.**

$P = 3.8 \times 10^{-10}$) in nondiabetic participants from the PPP-Botnia Study (Supplementary Table 1) (7). Of note, the number of individuals with measurements of LBM and fat percentage were fewer than those with information on BMI (2,826 vs. 4,468). On the contrary to plasma GIP concentrations, increased *GIPR* mRNA levels correlated negatively with BMI and waist circumference in the EUGENE2 and Danish Twins studies, as well as with visceral fat mass ($r = -0.53$, $P = 1 \times 10^{-6}$), but not with subcutaneous fat ($r = -0.11$, $P = 0.26$) measured by computed tomography in the EUGENE2 cohort (Supplementary Table 2). There was a weak inverse relationship between fasting plasma GIP concentrations and *GIPR* mRNA in adipose tissue ($n = 197$, $r = -0.155$, $P = 0.030$), especially in hyperglycemic (impaired fasting glucose and T2D) individuals ($n = 75$, $r = -0.342$, $P = 0.003$). This could be a corollary of the larger variation in GIP concentrations seen in hyperglycemic individuals.

Of twin pairs discordant for BMI (difference of >2 kg/m^2), the twin with lower BMI showed higher expression of *GIPR* in subcutaneous fat (0.243 ± 0.02 vs. 0.147 ± 0.01, $P = 0.001$) than the obese twin. Consequently, increased *GIPR* mRNA in adipose tissue correlated positively with insulin sensitivity assessed as rates of whole-body glucose uptake ($r = 0.39$, $P = 3 \times 10^{-5}$) and glucose oxidation ($r = 0.38$, $P = 7 \times 10^{-5}$) measured during a hyperinsulinemic-euglycemic clamp as well as with adiponectin concentrations ($r = 0.43$, $P = 2 \times 10^{-5}$) (Supplementary Table 2).

Effects of a variant in the *GIPR* gene (rs10423928) on body composition and metabolism. The A allele of a variant in the *GIPR* gene (rs10423928) was associated with lower BMI, fat, and LBM measured by bioimpedance (7), suggesting that the A allele is associated with reduced receptor function. The effect on LBM was replicated in 118 men measured by dual-energy X-ray absorptiometry showing that carriers of the A allele had a significant reduction in LBM of 2.88 kg (TT genotypes, 59.84 ± 6.53, vs. TA/AA genotypes, 56.95 ± 5.70 kg; $P = 0.006$) (Supplementary Table 3). The association of the A allele with reduced fat mass was also supported by a decrease in serum leptin levels in men from the Botnia study ($n = 484$, β [ln transformed] ± SEM, −0.039 ± 0.02; mean ± TT, 5.22 ± 0.24, TA 4.80 ± 0.22, AA 3.79 ± 0.34 μg/L, $P = 0.012$).

In an overfeeding study (12,13), GIP levels were significantly increased in homozygous TT carriers of *GIPR* rs10423928 (mean ± SD, 47.0 ± 17.1 vs. 90.7 ± 63.3 pg/mL; $P = 0.003$), but not in A-allele carriers (54.0 ± 22.5 vs. 65.7 ± 28.0 pg/mL; $P = 0.12$) (Supplementary Table 4). In 48 young healthy men, the *GIPR* SNP rs10423928 was associated with changes in substrate oxidation during high-fat feeding. In hyperinsulinemic-euglycemic clamp and indirect calorimetry, carriers of the insulin-reducing A allele showed a slightly lower rate of fat oxidation (TT, 1.15 ± 0.44, vs. TA/AA, 0.84 ± 0.40 mg/kg FFM/min; $P = 0.027$) and higher rate of glucose oxidation (TT, 1.98 ± 0.64, vs. TA/AA, 2.55 ± 0.97 mg/kg FFM/min; $P = 0.018$), suggesting a change in the availability of fatty acid substrates to the mitochondria and a subsequent increase in glucose utilization (Supplementary Table 4).

Although there was no eQTL (expression quantitative trait loci) effect of the *GIPR* rs10423928 genotype on total *GIPR* mRNA in SAT from 329 individuals (Supplementary Table 5*A* and *B*), we cannot exclude the possibility that the variant would influence expression of *GIPR* in a given individual in an allele-specific manner or its splicing pattern. A wide range of splice variants of *GIPR* was detected in SAT and VAT, of which only a few corresponded to the full-length (active) isoform (Fig. 1*B*). To investigate this further, we used a nonsynonymous coding SNP (rs1800437) in strong linkage disequilibrium with rs10423928 as a reporter SNP for quantitative allele-specific expression analysis in adipose tissue (SAT and VAT from 20 individuals). It is unlikely that the SNP would influence the total amount of *GIPR* mRNA in an allele-specific manner as there was at most a 10% difference in expression of the C and G alleles in heterozygous (G/C) carriers of the *GIPR* rs1800437 (Supplementary Fig. 2).

We next explored whether the rs10423928 SNP in the *GIPR* gene could influence the splicing pattern of *GIPR* in adipose tissue given that in mouse, there is clear evidence of alternative splicing of *GIPR* (18). Up to 64 possible variants were detected by RT-PCR and sequencing. Only two of these comprise the exons and splice sites predicted to yield a fully functional, membrane-bound GIPR, containing the intact NH_2-terminal hormone-binding domain as well as the complete seven-helix membrane-spanning domain (Fig. 1*C*). In adipose tissue from subjects with the A allele of SNP rs10423928 in the *GIPR* gene, a slight decrease in the proportion of splice variants containing exon 9, which is required for coding the transmembrane domain, was observed (Fig. 1*D*).

GIP stimulates OPN in adipose tissue. OPN has been shown to be markedly increased in adipose tissue from obese individuals and has been suggested to link obesity with systemic insulin resistance (2,3). In line with this, we observed that *OPN* expression was increased in adipose tissue from obese twins compared with their lean counterparts (mean ± SEM; $n = 86$, 0.13 ± 0.04 vs. 0.04 ± 0.01, $P < 0.05$). *OPN* mRNA correlated positively with BMI ($n = 196$, $r = 0.36$, $P = 3.1 \times 10^{-7}$) and negatively with insulin sensitivity ($n = 192$, $r = -0.24$, $P = 0.0008$), but the inverse correlation between *OPN* mRNA and insulin sensitivity was restricted to carriers of the A allele ($n = 39$, TA/AA, $r = -0.481$, $P = 0.002$ vs. $n = 44$, TT, $r = -0.056$, $P = 0.71$) (Fig. 2*A*). Carriers of the *GIPR* SNP rs10423928 TA/AA genotype had lower *OPN* expression in adipose tissue than TT genotype carriers ($P < 0.05$) (Fig. 2*B* and Supplementary Table 5*A*).

Notably, GIP stimulated OPN in isolated rat adipocytes incubated at high glucose in an insulin-dependent fashion ($P < 0.001$) (Fig. 2*C*).

DISCUSSION

The current study provides several novel insights into the role of GIP in the pathophysiology of obesity and type 2 diabetes by exploring a possible link between GIP, OPN, and insulin resistance. First, we confirm that increased OPN expression in human adipose tissue is associated with insulin resistance and obesity. Second, we present evidence that GIP stimulates OPN expression together with insulin in adipocytes, thereby contributing to adipose tissue inflammation characteristic of obesity and thus promoting insulin resistance. Third, a genetic variant with reduced GIPR function is associated with lower OPN and better insulin sensitivity.

OPN is one of the most abundant cytokines in adipose tissue from obese individuals where it specifically is localized in and around inflammatory cells and in adipocytes (3). We show here that GIP in a dose-dependent fashion in concert with insulin stimulates OPN expression in adipocytes, which in turn could contribute to the inflammation

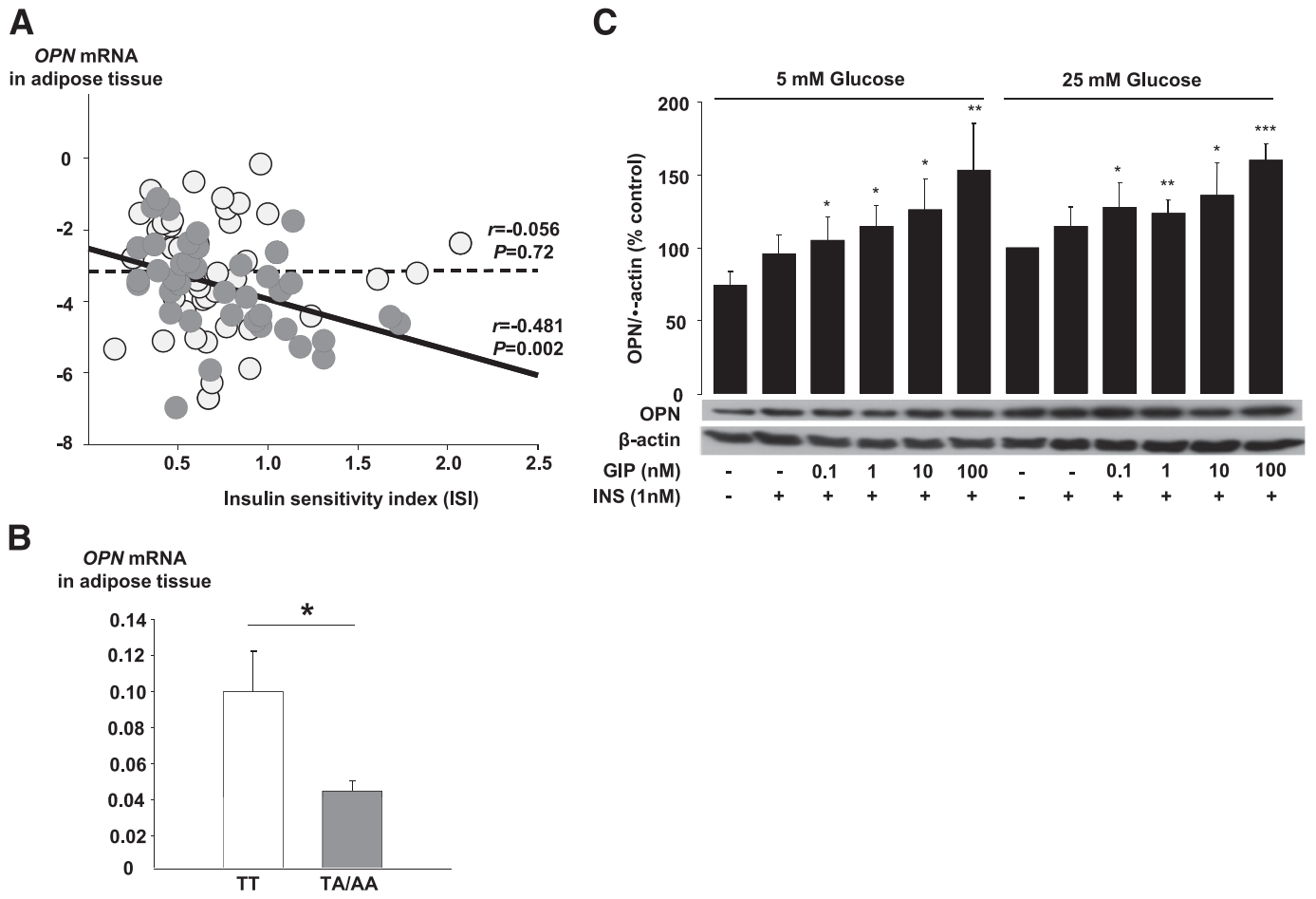

FIG. 2. Effects of GIP and *GIPR* genotype on OPN expression in adipocytes. *A*: Correlation between *OPN* mRNA in adipose tissue and ISI in different *GIPR* SNP rs10423928 carriers (Danish Twins Study, $n = 83$) (TT, black solid lines and gray circles; TA/AA, dashed lines and empty circles). *B*: Expression of *OPN* mRNA was lower in adipose tissue from TA/AA vs. TT genotype carriers (Danish Twins Study, *$P < 0.05$). *C*: GIP stimulation induces OPN in primary rat adipocytes. Adipocytes were isolated from rat epididymal fat pads and incubated overnight (~18 h) in media containing either 5 or 25 mmol/L glucose in the presence of GIP and insulin at the indicated concentrations. Data are presented as mean ± SEM of OPN protein expression relative to β-actin, expressed as percent of control cell (25 mmol/L glucose) expression. $n = 6–12$ per condition. *$P < 0.05$; **$P < 0.01$; ***$P < 0.001$.

and insulin resistance characteristic of obesity. Importantly, these effects were seen acutely and would therefore be independent of expansion of adipose tissue. Although data in rodents strongly support the view that inhibition of OPN improves insulin sensitivity, data in humans are merely of associative character, where OPN expression in adipose tissue was inversely correlated with measures of total-body insulin sensitivity. In addition, it has been shown that inhibition of OPN by a neutralizing antibody reduced inflammation in adipose tissue and liver in diet-induced obese mice (19). It may not be feasible to use such antibodies in humans, but our data suggest that similar effects can be achieved by reducing GIP effects in adipose tissue as carriers of the A allele in the *GIPR* variant had lower OPN expression in adipose tissue as well as reduced body weight, which also included reduced abdominal fat. Since GIP stimulates adipose tissue formation independently of its effect on insulin secretion, inactivation of GIPR in adipose tissue has been suggested as a strategy to treat obesity (5). Our data suggest that it might also improve insulin sensitivity. There was also higher expression of *GIPR* transcript observed in visceral as compared with subcutaneous fat in a group of obese nondiabetic subjects undergoing bariatric surgery. However, we could not exclude the possibility of a confounder effect, as unfortunately, similar samples were not available from the general population, and this could thus be specific to morbidly obese individuals.

As alternative splicing of the *GIPR* results in isoforms with both stimulatory and inhibitory properties in mice (18), we also studied whether there would be allele-specific effects on splicing that could explain the reduced effect of GIP in adipose tissue. Our data suggest that this could be a possible scenario as carriers of the A allele showed a lower amount of the exon 9–containing isoform, which is required for transmembrane activity. Given the small number of individuals with information on splicing pattern, it would be necessary to obtain not only replication in additional samples but also information on *GIPR* mRNA splicing in different tissues.

In conclusion, we describe a link between GIP and OPN in adipose tissue that could link GIP to insulin resistance (Fig. 3). Exactly what mechanisms mediate this effect are not known; however, our recently published data indicate a role for the transcription factor nuclear factor of activated T cells since the effect of GIP on OPN expression could be inhibited by a blocker of nuclear factor of activated T cells (20). From a therapeutic point of view, it

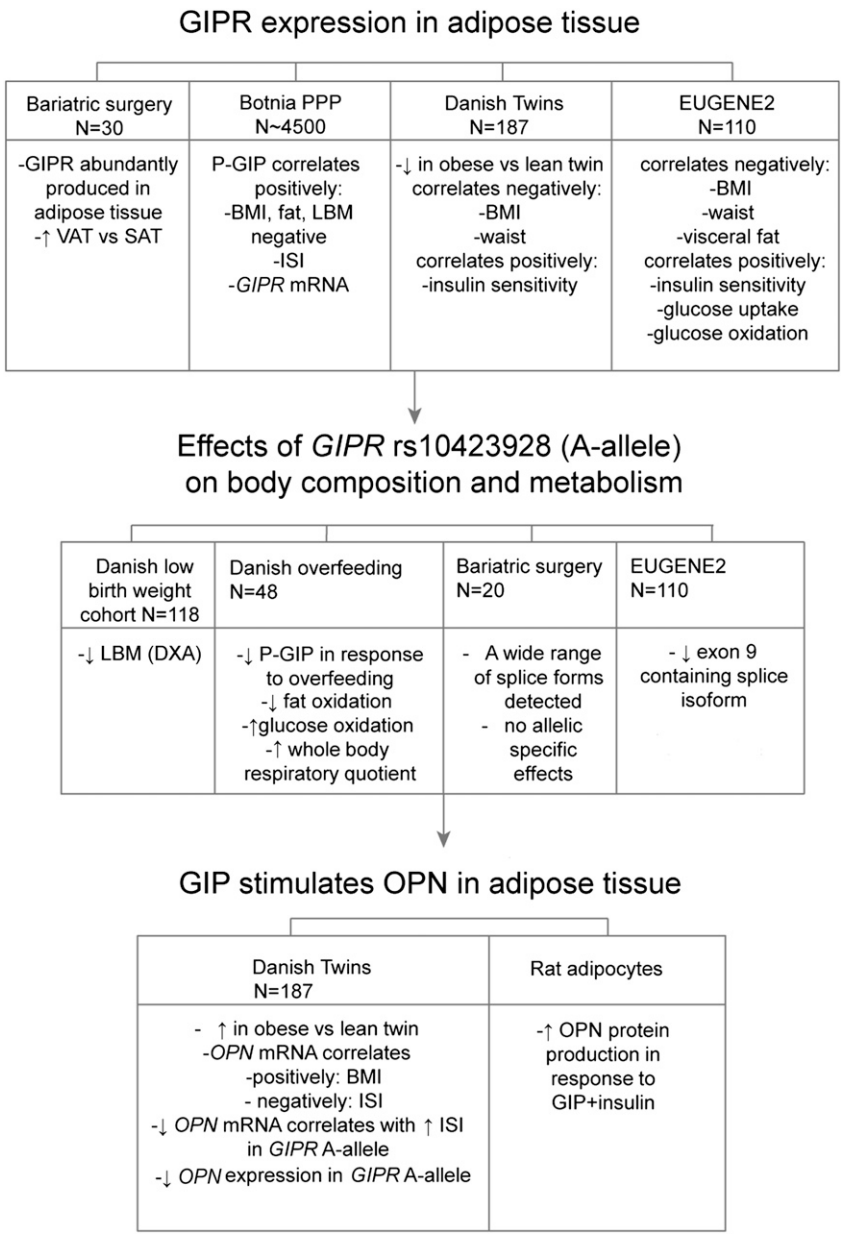

FIG. 3. Diagram of the design and summary of the study. DEXA, dual-energy X-ray absorptiometry. P-GIP, plasma-GIP.

would be important to characterize different GIPR splice isoforms in different human tissues to obtain information on their activating/inactivating properties.

ACKNOWLEDGMENTS

The studies at Lund University were supported by a Linnaeus grant (LUDC) (Dnr. 349-2008-6589), the Swedish Research Council including project grants (Dnr. 521-2007-4037 to L.G. and Dnr. 521-2010-2633 to V.L.), a strategic research area grant (EXODIAB, Dnr. 2009-1039), an advanced research grant from the European Research Council to L.G. (GA 269045), equipment grants from Wallenberg (KAW 2009-0243) and the Lundberg Foundation (Grant 359), and grants from the following foundations: Novo Nordisk, Åhlén, Åke Wiberg, Magnus Bergwall, Tore Nilsson, Fredrik and Ingrid Thuring, Crafoord, Albert Påhlsson, Lars Hierta Memorial, Royal Physiographic Society, the Foundation of the National Board of Health and Welfare, Malmö University Hospital, and the European Foundation for the Study of Diabetes. Work in Kuopio, Finland, was supported by grants from the Academy of Finland and the Finnish Diabetes Research Foundation. In addition, the project was funded by the European Union grant ENGAGE.

No potential conflicts of interest relevant to this article were reported.

E.A. performed data analyses and genotyping and drafted the report. P.O., T.K., O.K., A.V.Z., O.H., and J.P. performed expression experiments in adipose tissue. K.P., C.B., and P.P. performed incretin clamp and expression in adipose tissue experiments. B.O. and E.D. performed in vitro experiments in adipose tissue. A.S. and J.K. performed phenotyping and data analyses in the EUGENE2 Study. A.J. performed genotyping and genetic data analyses.

T.J.K. provided GIP antibodies. T.T. and B.I. performed phenotyping in the Botnia study. S.M. and A.V. were the principal investigators of the Danish studies. M.F.G. performed expression and in vitro experiments in adipose tissue and designed the study. M.L. was the principal investigator of the EUGENE2 study. N.W. performed immunocytochemistry. L.G. designed the study and drafted the report. V.L. performed genetic data analysis, designed and supervised all parts of the study, and drafted the report. All researchers took part in the revision of the report and approved the final version. L.G. is the guarantor of this work and, as such, had full access to all the data in the study and takes responsibility for the integrity of the data and the accuracy of the data analysis.

The authors thank Britt-Marie Nilsson (Department of Clinical Sciences, Islet cell exocytosis, University Hospital Malmö, Malmö, Sweden), Mona Svärdh (Department of Clinical Sciences, Diabetes and Endocrinology, University Hospital Malmö, Malmö, Sweden), Esa Laurila (Department of Clinical Sciences, Diabetes and Endocrinology, University Hospital Malmö, Malmö, Sweden), Anna Berglund (Department of Clinical Sciences, Diabetes and Endocrinology, University Hospital Malmö, Malmö, Sweden), Malin Neptin (Department of Clinical Sciences, Diabetes and Endocrinology, University Hospital Malmö, Malmö, Sweden), Doris Persson (Department of Clinical Sciences, Unit of Neuroendocrine Cell Biology, University Hospital Malmö, Malmö, Sweden), and Anna-Maria Veljanovska-Ramsey (Department of Clinical Sciences, Islet cell exocytosis, University Hospital Malmö, Malmö, Sweden) for technical support.

REFERENCES

1. Gustafson B. Adipose tissue, inflammation and atherosclerosis. J Atheroscler Thromb 2010;17:332–341
2. Nomiyama T, Perez-Tilve D, Ogawa D, et al. Osteopontin mediates obesity-induced adipose tissue macrophage infiltration and insulin resistance in mice. J Clin Invest 2007;117:2877–2888
3. Pietiläinen KH, Naukkarinen J, Rissanen A, et al. Global transcript profiles of fat in monozygotic twins discordant for BMI: pathways behind acquired obesity. PLoS Med 2008;5:e51
4. Singh M, Ananthula S, Milhorn DM, Krishnaswamy G, Singh K. Osteopontin: a novel inflammatory mediator of cardiovascular disease. Front Biosci 2007;12:214–221
5. Miyawaki K, Yamada Y, Ban N, et al. Inhibition of gastric inhibitory polypeptide signaling prevents obesity. Nat Med 2002;8:738–742
6. Yamada C, Yamada Y, Tsukiyama K, et al. Genetic inactivation of GIP signaling reverses aging-associated insulin resistance through body composition changes. Biochem Biophys Res Commun 2007;364:175–180
7. Lyssenko V, Eliasson L, Kotova O, et al. Pleiotropic effects of GIP on islet function involve osteopontin. Diabetes 2011;60:2424–2433
8. Isomaa B, Forsén B, Lahti K, et al. A family history of diabetes is associated with reduced physical fitness in the Prevalence, Prediction and Prevention of Diabetes (PPP)-Botnia study. Diabetologia 2010;53:1709–1713
9. Matsuda M, DeFronzo RA. Insulin sensitivity indices obtained from oral glucose tolerance testing: comparison with the euglycemic insulin clamp. Diabetes Care 1999;22:1462–1470
10. Poulsen P, Kyvik KO, Vaag A, Beck-Nielsen H. Heritability of type II (non-insulin-dependent) diabetes mellitus and abnormal glucose tolerance—a population-based twin study. Diabetologia 1999;42:139–145
11. Poulsen P, Vaag A, Beck-Nielsen H. Does zygosity influence the metabolic profile of twins? A population based cross sectional study. BMJ 1999;319:151–154
12. Brøns C, Jacobsen S, Hiscock N, et al. Effects of high-fat overfeeding on mitochondrial function, glucose and fat metabolism, and adipokine levels in low-birth-weight subjects. Am J Physiol Endocrinol Metab 2012;302:E43–E51
13. Frayn KN. Calculation of substrate oxidation rates in vivo from gaseous exchange. J Appl Physiol 1983;55:628–634
14. Laakso M, Zilinskaite J, Hansen T, et al.; EUGENE2 Consortium. Insulin sensitivity, insulin release and glucagon-like peptide-1 levels in persons with impaired fasting glucose and/or impaired glucose tolerance in the EUGENE2 study. Diabetologia 2008;51:502–511
15. Wang J, Kuusisto J, Vänttinen M, et al. Variants of transcription factor 7-like 2 (TCF7L2) gene predict conversion to type 2 diabetes in the Finnish Diabetes Prevention Study and are associated with impaired glucose regulation and impaired insulin secretion. Diabetologia 2007;50:1192–1200
16. Honnor RC, Dhillon GS, Londos C. cAMP-dependent protein kinase and lipolysis in rat adipocytes. I. Cell preparation, manipulation, and predictability in behavior. J Biol Chem 1985;260:15122–15129
17. Lewis JT, Dayanandan B, Habener JF, Kieffer TJ. Glucose-dependent insulinotropic polypeptide confers early phase insulin release to oral glucose in rats: demonstration by a receptor antagonist. Endocrinology 2000;141:3710–3716
18. Harada N, Yamada Y, Tsukiyama K, et al. A novel GIP receptor splice variant influences GIP sensitivity of pancreatic beta-cells in obese mice. Am J Physiol Endocrinol Metab 2008;294:E61–E68
19. Kiefer FW, Zeyda M, Gollinger K, et al. Neutralization of osteopontin inhibits obesity-induced inflammation and insulin resistance. Diabetes 2010;59:935–946
20. Omar B, Banke E, Guirguis E, et al. Regulation of the pro-inflammatory cytokine osteopontin by GIP in adipocytes—a role for the transcription factor NFAT and phosphodiesterase 3B. Biochem Biophys Res Commun 2012;425:812–817